Prediction of streetwise AQI from deposited pollutant on leaf Phyllotaxy using Vision transformer and FTIR Spectral data

Graphics Abstract

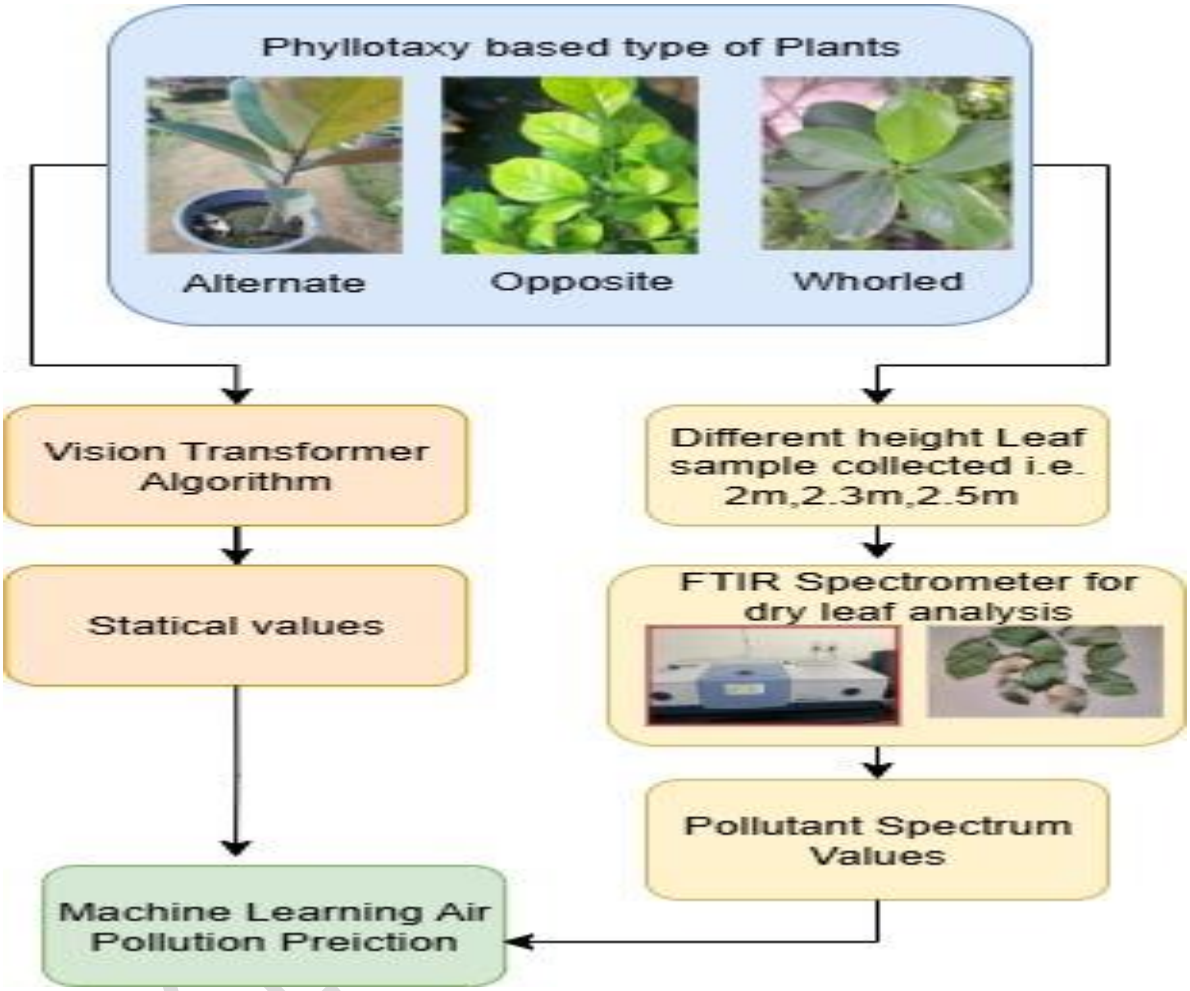

Highlights

- Air pollutant deposition is measured from leaf phyllotaxy.
- Analyse dry leaf samples for pollutant deposition using FTIR spectroscopy.
- Pollutant deposition spectrum data and laborators collected pollution values are correlated with machine learning and prediction of AQI.
- Leaf-based spectral pollutant deposition data and visual analysed pollutant deposition data after processing with ViT are used for AQI prediction.
- AQI measured for streetwise and analysis how traffic leads to high deposition of pollutant through phyllotaxy pollutant deposition data,leaf pollutant image data,and laboratory based pollutant data.

Abstract

Urban air pollution need to be measured on streetwise and not the area -wise.The World Health Organisation reports that 99% of people worldwide breathe air that is beyond WHO standards, and that air pollution results in more than 7 million preventable deaths each year (WHO, 2023). In existing, area-wise pollutant/AQI is measured and not the streetwise AQI. By monitoring the leaf deposition on trees that are directly next to each street, a streetwise technique can identify micro-scale variations in deposition that are highly correlated with pedestrian exposure and local traffic volume..To solve the above problem,Phyllo-ViT method is proposed for streetwise AQI measurement. Phyllo-ViT is a multi-modal leaf sensing system that uses ViT to extract morphological patterns from photos, FTIR spectra to offer chemical fingerprints of deposited VOCs and inorganic species, and leaf images to provide visual indications of particulate deposition. A more reliable predictor of local AQI is produced when these modalities are combined than when they are used separately. The Vision Transformer (ViT) extracts, the pollutant from leaf image. Phyllo-ViT provides a scalable and non-invasive substitute for existing sensor-based system for predicting the Air Quality Index (AQI). The combination of artificial intelligence, spectroscopy, and plant physiology are used for measuring the pollutant on streetwise in real time.The results of phyllo-ViT model is compared with the standard metrics. The proposed Phyllo-ViT model achieves the highest accuracy in street residential low traffic areas R^2 of about 0.96 and the lowest accuracy in high traffic areas with an R^2 of about 0.93.

Keywords: Air Pollution, FTIR , Machine Learning, Vision Transformer, AQI, Pollutants, Prediction

1. Introduction

To measure the amount of pollutants in the air on daily basis for an area703 monitoring stations has been placed throughout Indian cities. Massive emissions of dust and gases into the atmosphere is due to the rapid industrial and commercial expansion and lead to low air quality. Human wellness, environmental degradation, and ecology are all negatively impacted by air pollution. The quality of the air has been declining daily due to both natural and man-made factors. Due to the rise in industrial pollutants and traffic, as well as the decline in vegetation, the air quality in the world's largest cities have been steadily declining. Since 95% of Indians and 99% of people worldwide [1] reside in regions with air pollution levels above WHO standards, it is a major worldwide concern.

The increase in pollutant contaminants in the air such as sulfur, carbon, and nitrogen oxides have a significant impact on the environment, growing areas, and humans. Reducing air pollution plays a vital role as an important goal. The plants act as air filter, the air by bio-filtering the pollutants through absorption, impingement, and adsorption [2, 3], improves the soil and water quality of the area in addition to adding aesthetic value [4]. Green cover along the roadside has garnered a lot of attention because it is an economical and environmentally friendly filter for reducing air pollution levels [5]. Plants absorb gaseous pollutants through gaseous exchange and particle pollutants through wet and dry deposition on the leaf surface [6]. Although the leaves are the main absorbers of air pollutants, their responses various based on types of plants air pollutants [7]. Furthermore, pollutants on plants leaf weather factors such as wind and rainfall lead to movement of air pollutants. Dust deposition varies among plant species due to

factors such as leaf orientation, leaf surface geometry, phyllotaxy, epidermal and cuticular characteristics, leaf pubescence, height, and canopy of roadside plants. The plant dust accumulation differ depending on the plant species [8]. The roadside plant changes its morphological and physiological characteristics in an adaptive reaction to the dust deposition. In this study, leaves on a stem as phyllotaxy displays a distinct leaf arrangement. There are four types of leaves: whorled, opposite, spiral, and alternate.

In India, FTIR spectroscopy is frequently used to identify the kind of pollutants such as gaseous, liquid, or solid and monitor the effects of pollution [9]. The spectral-chemical composition of the pea leaf cuticle at the onset of flowering is measured using ATR-FTIR spectroscopy in conjunction with uni- and multivariate analysis, specifically the effects of variety, heat stress, and growth environment [10].In this paper phyllotaxy and vision transformer is tunning with machine learning to predict air pollutants in the streetwise . The main aim of this work is

- To develop and analyze Phyllo-ViT, a multimodal approach that predicts streetwise AQI and pollutant concentrations using roadside tree leaf photos (phyllotaxy), FTIR spectral measurements, and official AQI records.

The Objective, Motivation & Scope of the proposed work is provided below as follows:

- (1) Arrange matched leaf images, FTIR spectra, and CPCB (HPCB) AQI data at the street level; (2) extract chemical features from FTIR and morphological features (contrast, entropy, and std) from leaf images; (3) train and validate a Vision Transformer (ViT)-based model fused with regression (BO-MLR) for pollutant prediction; (4) compare Phyllo-ViT against baseline methods and report R^2 RMSE, MAE, and classification metrics; (5) explore practical deployment and limitations.

- Motivation arises from the poor spatial resolution of area-wise AQI for street exposures; scope is limited to roadside tree leaves in two study regions (Vatika Sector-82, Gurugram and IMT Manesar), data collected March 2025, and pollutants PM2.5, PM10, NO2, CO, and O3.

Phyllotaxy leaves used for pollutant deposits on the leaf and improve the pollutant prediction accuracy.The pollutant in the air is deposited on leaf and from image of leaf extracted the pollution from the pixels of leaf region. The proposed Phyllo-ViT model are used in this paper to measure air pollutant prediction using tree leaf. The contributions of this paper are as follows:

1. To predict air pollutant levels using roadside tree leaves collected from high traffic and low traffic residential areas.
2. To analyse pollutant deposition on roadside tree leaves using FTIR spectroscopy.
3. To predict the Air Quality Index (AQI) by extracting streetwise roadside tree leaf images using high-resolution cameras, where pollutant deposition based on phyllotaxy is analysed through a Vision Transformer (ViT) at the pixel level.

To predict and forecast air pollution levels using tree leaves from high-traffic and low traffic residential areas by jointly analysing phyllotaxy, FTIR values, pixel level features from leaf images, and AQI values obtained from HPCB.

The rest of the paper is structured as below. Section II explain about literature review. The ViT algorithm and its approach to air quality prediction is explained in Section III. The experimental

setup and methodology are demonstrated in Section IV. The findings are presented in Section V. The research is discussed in Section VI, and the model Phyllo-ViT is tunned with machine learning for the prediction of air contaminants on tree leaves are concluded in Section VII.

2. Literature Review

Research on urban air contaminant levels, sources, and health impacts have steadily increased during the last ten years [11]. The length of pedicles, the quantity of flowers in an inflorescence, and seed germination are all impacted by air pollutants [12]. The plant species can be utilized as a bio-monitor to assess the effects of air pollution. Soil acidification is an indirect effect of air pollution, leaves are a direct indicator of air pollutant deposition [13]. The vehicle exhaust on roadside affects vegetation [14]. Air Pollution Tolerance Indices (APTI) of four plant species cultivated alongside a road in a polluted location were compared with those of an unpolluted garden area [15].

Studies on roadside deposition conducted worldwide have shown that large amounts of pollutants are deposited on plants in China [16] and India [17], which has highlighted the high concentrations of PM, gaseous pollutants, and heavy metals that accumulate in plants. Road dust is resuspended in the atmosphere by wind and vehicle movements on roadways and has a dynamic connection with the ground-level atmosphere [18, 19]. Based on estimates of PM10/TSP ratios for various sources, the Urban Air Quality Management Strategy in Asia (URBAIR) discovered that road dust resuspension accounted for 20% of atmospheric PM10 [20]. Numerous studies have documented a significant decline in plant physiology as a result of dust [21, 22].FTIR is used in numerous investigations pertaining to air pollution.

Numerous investigations of air pollution have used FTIR in environmental chambers and ambient air [23, 24]. Using TG-FTIR, the researcher investigated the pyrolysis of three different willow sample types that were taken from the leaves, stems, and branches of the plant. Numerous studies have been conducted on this effect [25]. In certain situations, a leaf's capacity to reflect sunlight and regulate water loss might be a component of the stress response. If ATR-FTIR spectroscopy used to identify such variations in the leaf surface, which is a quick method to look at how heat stress alters the leaf cuticle and then determine, which tree species are heat-sensitive and heat-tolerant [26]. Researchers have not recorded CO, CO2, and N2O or NH3 emissions from busy roadside locations [27].

The study provides a thorough evaluation of machine learning approaches for Air Quality Index (AQI) prediction using pollutant and meteorological data from Iğdır, Türkiye. By comparing SVM, LightGBM, and XGBoost models, the authors demonstrate that ensemble-based methods, particularly XGBoost, significantly outperform traditional approaches, achieving near-perfect predictive accuracy with low error metrics, indicating strong capability in modeling complex, multidimensional relationships[28].Using the "Broadband China" project as a natural experiment, this study demonstrates how the growth of the digital economy considerably lowers PM2.5 levels and AQI values throughout Chinese cities[29].The study offers an effective and scalable system for real-time AQI categorization based on important pollutant concentrations like CO, NO_2, O_3, and PM_2. by combining a robust preprocessing pipeline with curvature-aware optimization[30].The study shows that the RNN-PBO framework outperforms standalone neural network models and conventional machine learning techniques, offering a more reliable

and flexible approach for predicting important air contaminants in intricate urban settings. The results demonstrate that air-quality forecasting capabilities is greatly improved by combining meteorological data with sophisticated ensemble learning, providing a useful instrument for environmental monitoring and decision-making in urban environments[31].Wang et al. (2024) provide comprehensive empirical evidence from Chinese provincial panel data (2012–2022), demonstrating that digital financial inclusion significantly suppresses agricultural carbon emission intensity. Their findings suggest that digital finance improves access to credit, optimizes resource allocation, and accelerates the adoption of green agricultural technologies, thereby reducing carbon emissions [32].These plant-based indicators offer a cost-effective and environmentally sustainable alternative to conventional air-quality monitoring systems, particularly in urban and semi-urban regions where dense sensor deployment is challenging[33].However, existing studies are largely limited to laboratory analysis and descriptive statistical evaluation, restricting real-time applicability and large-scale deployment. Consequently, recent literature highlights the need to integrate plant-derived features with advanced computational and machine-learning frameworks to enhance prediction accuracy, scalability, and real-time air-quality assessment.

Problem Statement

In India, pollutants are measured i.e AQI in area-wise and not street-wise. The traffic volume and pollutant deposition on that area with AQI need to be measured.AQI on the roads are not measured. The measurement of AQI in streetwise help the environment engineers to plan the trees to be planted on the roadsideSome of the limitations of current research include Initially, deep learning models (like CNNs) that are trained on photos from one region frequently don't work well when used in another because of variations in the terrain, traffic, building density, or atmospheric conditions. Likewise, temporal variations (such as seasonality, policy modifications, or anomalous occurrences) impair model performance.When used outside of the region or time period in which they were trained, these models' performance declines, frequently exhibiting poor spatial and temporal generalization [34]. Second, because street-view imagery is more commonly used in high-traffic regions and residential and green spaces are under-represented, it adds coverage bias [35]. Third, the accuracy of predictions is extremely sensitive to environmental factors and image quality; low light, rain, or poor vision can skew visual features and produce estimations that are not trustworthy [36].

Leaf arrangement influence pollutant capture. Phyllotaxy is the arrangement of leaves on a stem. More exposure area on plant surface is required for pollutant trapping such as dust,PM2.5,PM10 and heavy metal. Measuring pollutant deposition linked with phyllotaxy shows,which plant geometries are best for accurate AQI measurement. Tranditional AQI sensors measures air quality at a point. Plant leaf deposition studies reflect cumulative pollution exposure over a time.

Phyllotaxy based AQI measurement is cost effective and eco-friendly AQI monitoring.Instead of inserting expensive instruments everywhere, plants with favourable phyllotaxy can be used as biomarker. This phyllotaxy based AQI measurement avoid the dense AQI sensors

networks.The amount of pollutant deposition is proportional to local air quality due to pollutant deposits on plants for long term.

Street-wise AQI measurement leads to acquire local pollution hotspot.Street-wise AQI helps for urban planning and traffic manegment i.e. humans can avoid certain routes or travel off-peak hours.Street-wise AQI helps humans to know which areas are safer to walk,jog or cycle.Hospitals and schools can be advised to limit outdoor activities during poor AQI hours.Street-wise AQI,helps for green corridors with pollution absorbing trees.Street-wise AQI helps to identify low-emision zones,which helps asthma,COPD and heart patients.

3. Methodology

This section explains the model used for the prediction of air pollutants. This study aims to use various methods, such as phyllotaxy-based outdoor plant leaf images, FTIR spectrum values from dry leaves, and Central Pollution Control Board values to predict AQI on streetwise.The overview of this study is depicted in Fig. 1.

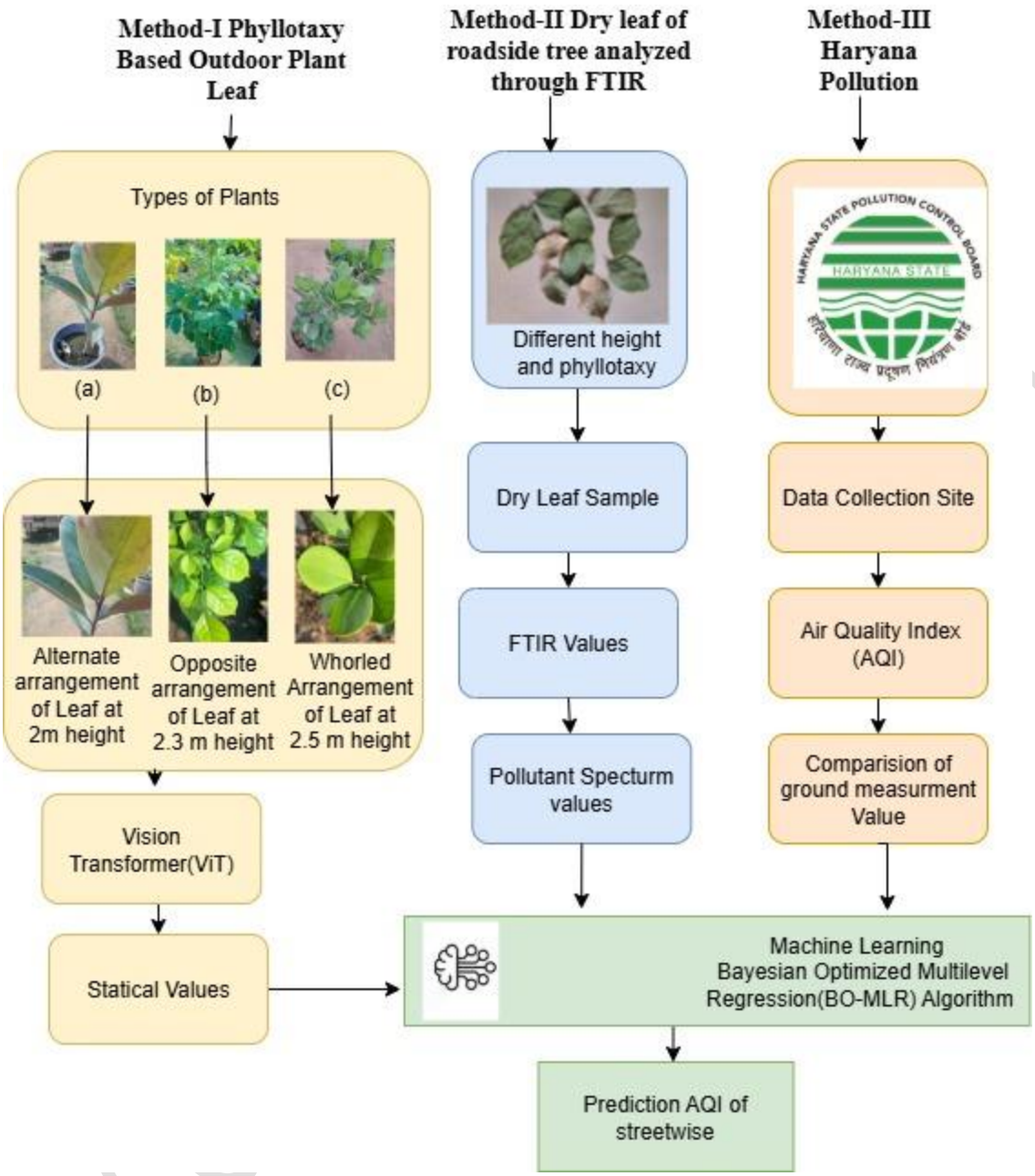

Figure1: Proposed a Model Phyllo-ViT (Phyllotaxy Vision Transform Model for Air Pollution Prediction using Machine learning)

Method 1: Phyllotaxy leaf based outdoor plant leaf images are used for predict AQI in high-traffic and residential low traffic areas.
Method 2: FTIR was used to check for pollutant deposition levels in the dry leaves of roadside plants.
Method 3: Air Quality Index data from the Haryana Pollution Control Board (HPCB) are collected with the data obtained from above method I and method II.

The studied regions are Vatika-secttor 82 in Gurugram and IMT Manesar. National Air Quality Index (NAQI) stations' air quality (AQ) data are gathered in the aforementioned locations. IMT Manesar is highly polluted. At a precise height of 2.5 meters, leaves were gathered from phyllotaxy based trees in both residential low-traffic and high-traffic locations. The air pollutants are measured from the spectrometer values of dry leaf. Air pollution affects the vast majority of people on the planet. Humans breathe in harmful gases daily,so need to measure their level of AQI on streetwise.Figure 2 is the theoretical framework combines chemical, optical, and environmental data to use roadside tree leaves as bio-indicators for air quality assessment. FTIR spectroscopy is used to measure pollutant deposition in leaf samples taken from high- and low-traffic regions, and high-resolution imaging is used to extract phyllotaxy and stress-related characteristics. For supervised learning, official AQI data from the Haryana Pollution Control Board is combined with these plant-derived markers. Accurate air pollution level and AQI forecasts are made possible by the integrated machine learning model, which supports an economical and environmentally friendly method of air quality monitoring.

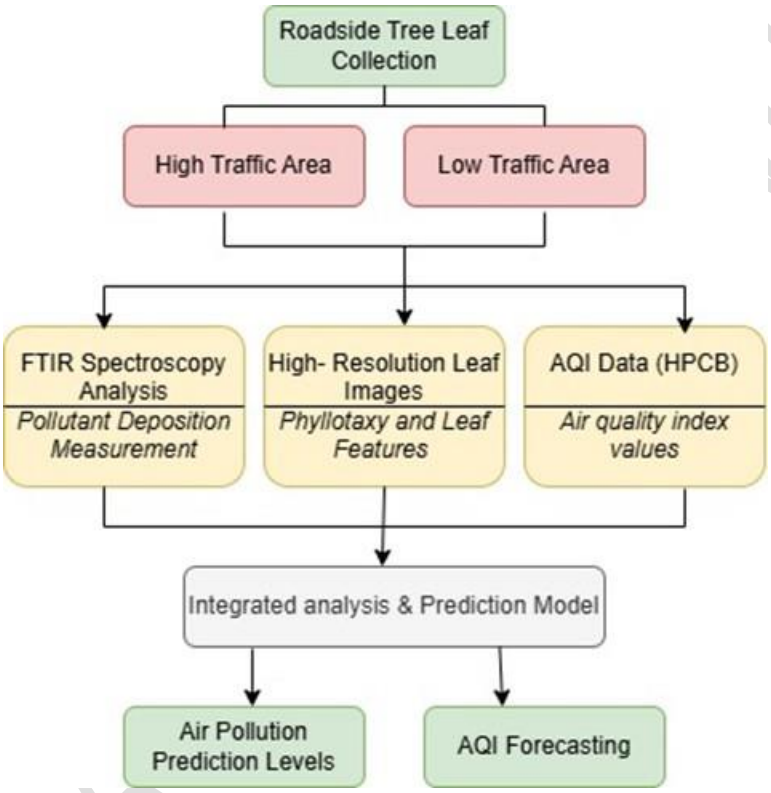

Figure 2: Proposed Model Phyllo-ViT (Phyllotaxy Vision Transform Model for Air Pollution Prediction using Machine learning) theoretical framework

4. Description of Experimental set-up

Method 1: Phyllotaxy-based outdoor plant leaf images are used for prediction of AQI in high-traffic and residential low-traffic areas.

The plant absorbs gaseous contaminants through gas exchange and particle pollutants through wet and dry deposition on the leaf surface [6]. The usage of phyllotaxy was utilised to arrange

the leaves on a branch. The species of a plant determines the quantity and arrangement of the leaves, with each species displaying a distinct leaf arrangement. There are four types of leaves such as whorled, opposite, spiral, and alternate. The outdoor test bed plant are used for measurement of pollutant contaminants deposition on the leaves in Figure 3. During peak hours of evening, the plant sapling is kept on the street road near low and high-traffic areas.

Figure 3: In outdoor high and low traffic areas on road test

For pixel in the leaf image, the pollutant deposition is measured after processing with ViT contrast,entropy and standard deviation are calculated. In contrast, entropy and standard deviation are computed independently for the IMT Manesar, and Vatika sector-82 research areas.

Method 2: Dry leaves from Roadside trees were analyzed through FTIR for pollutants.

The current section deals with dry leaves that were gathered from the IMT Manesar area, where Method- I previously analysed the DN for pollutants after processing with ViT algorithm. The FTIR instrument's photograph of the leaf sample testing area is displayed in figure 4. The spectrum output of dry leaf samples are obtained using FTIR, so measured pollutant deposition leaves and forecast air quality as in figure5. To prevent light and stray radiation, collected leaf samples are kept in a closed atmosphere beneath the sample slot. Condition such as liquid, solid, or powder of the samples are carried by the sample platform, which is made of quartz, glass, or plastic.

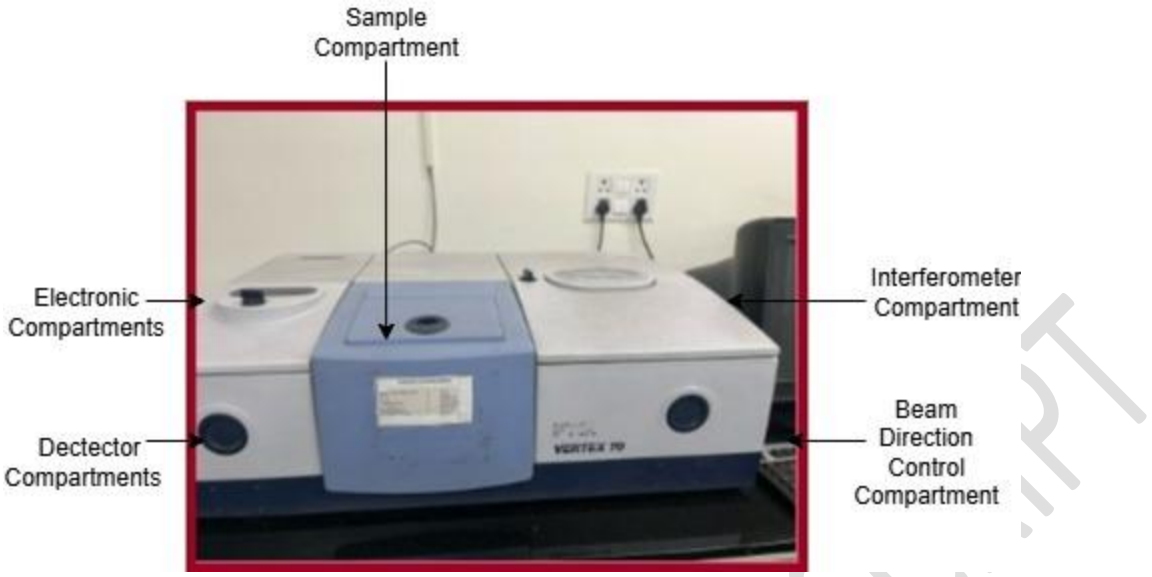

Figure 4: General FTIR Spectrometer view

Leaf samples were collected from the branches of street-facing trees from different heights, which are near to residential sides of the Aegle marmelos tree, leaf samples were collected in the evening peak hours. After being dried, the leaves are kept in plastic bags. For the purpose of measuring pollutants, the conserved samples were examined using FTIR

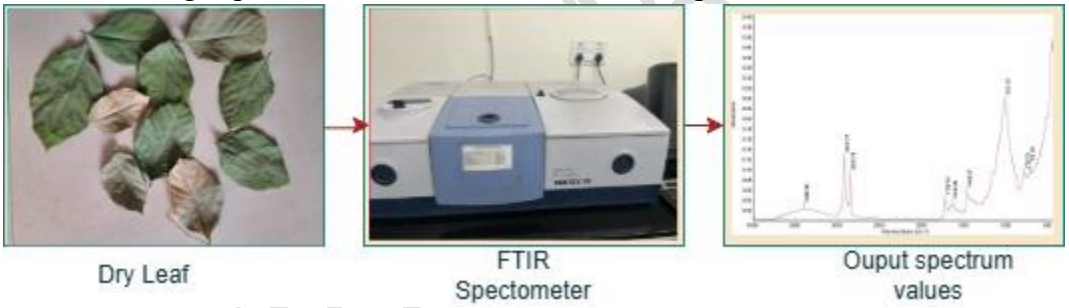

Figure 5: FTIR Spectrophotometer dry leaf sample output

The experimental setup and data acquisition details are summarized as follows in table I. Leaf biochemical analysis was carried out using an FTIR spectrometer model: Y- IR500 FTIR (400–4000 cm^{-1} range). Leaf imaging was performed using a high-resolution smartphone camera Samsung Galaxy Z fold6(50 MP) — Auto mode, ISO 100, 1/250 s exposure,with image resolution 1856 x 2160 pixels (~374 ppi density). Leaf samples were collected at a height of approximately 2.5 m during evening peak hours from two urban locations, namely Vatika Sector-82 (Gurugram) and IMT Manesar, as already described in methodology section. Model training and inference were conducted on a personal computer with a CPU Intel® Core™ i7-14700F Desktop Processor 20 cores (8 P-cores + 12 E-cores) up to 5.4 GHz and 32 GB RAM. The software environment included MATLAB R2024a with Deep Learning and Image Processing Toolboxes for Vision Transformer and Bayesian Optimization routines. In this study used publicly available CPCB/HPCB air quality data were integrated with offline FTIR measurements and smartphone-captured leaf images.

Table I:Detail of software and hardware used in experiment set-up

Category	Component / Device	Specification Detail
Hardware	Desktop Workstation	Intel® Core™ i7-14700F Desktop Processor 20 cores (8 P-cores + 12 E-cores) up to 5.4 GHz
	GPU	NVIDIA RTX 3060 (12 GB VRAM)
Software Environment	Operating System	Windows 11 Pro (64-bit)
	MATLAB	R2024a with Deep Learning and Image Processing Toolboxes
Spectroscopy Instrument	FTIR Spectrometer	*Model:* Y- IR500 FTIR (400–4000 cm^{-1} range)
	Sample Preparation	Dried leaf powder pelletized with KBr for FTIR scan
Imaging Device	Camera	Samsung Galaxy Z fold6(50 MP) — Auto mode, ISO 100, 1/250 s exposure
	Image Resolution	1856 x 2160 pixels (~374 ppi density)
Network Devices	Internet Connectivity	Fiber Broadband (100 Mbps download / 40 Mbps upload)
	Cloud Storage	Google Drive & MATLAB
Power and Environment	Supply	Constant 230 V AC, UPS backup for 1 hour
Dataset Sources	CPCB Portal (India)	https://airquality.cpcb.gov.in/AQI_India/

The pollutant spectrum of leaves collected from high-traffic and residential low-traffic areas along the road is displayed in figures 6 and figure 7.The plots display absorbance (A) on the y-axis and wave number (cm^{-1}) on the x-axis. Air pollutant absorption and transmission are reflected in the band amplitude. FTIR provides comprehensive information about the air contaminants, such as VOC, NH3, NO2, SO2, CO, and CH4 groups, by identifying certain bonds or spectrum regions.In Figure 5 and Figure 6, the Infra Red (IR) spectrum is divided into four areas.

In the first region, the wavenumber (cm^{-1}) is between 4,000 and 2,800; in the second, it is between 2,800 and 1,465; in the third, it is between 1,465 and 1,000; and in the fourth, it is between 1,000 and 500 (cm^{-1}). Every spectrum has a peak with distinct characteristics. The range of the IR group of functions is 4000 and 779.73 cm^{-1}.Every time the sample has contact with the infrared frequency, the infrared spectrum is created and prepared for additional confirmation. By generating a range of bond absorptions, functional groups aid in the interpretation of infrared spectra at various locations and strengths. The surface area of the fingerprint ranges from 1515 to 700 cm^{-1}. The primary emphasis of a molecule is molecular absorption by FTIR. Molecule that absorbs infrared light can induce stretching and bending effects, which often change the vibration and dipole of the bond. Spectrum correlation is the

term used to describe the consistent patterns that these effects produce with pollutant spectrum readings for each leaf sample. Certain vibrations observed in stretching and bending actions are crucial for defining their characteristics and distinguishing the molecule and functional group.

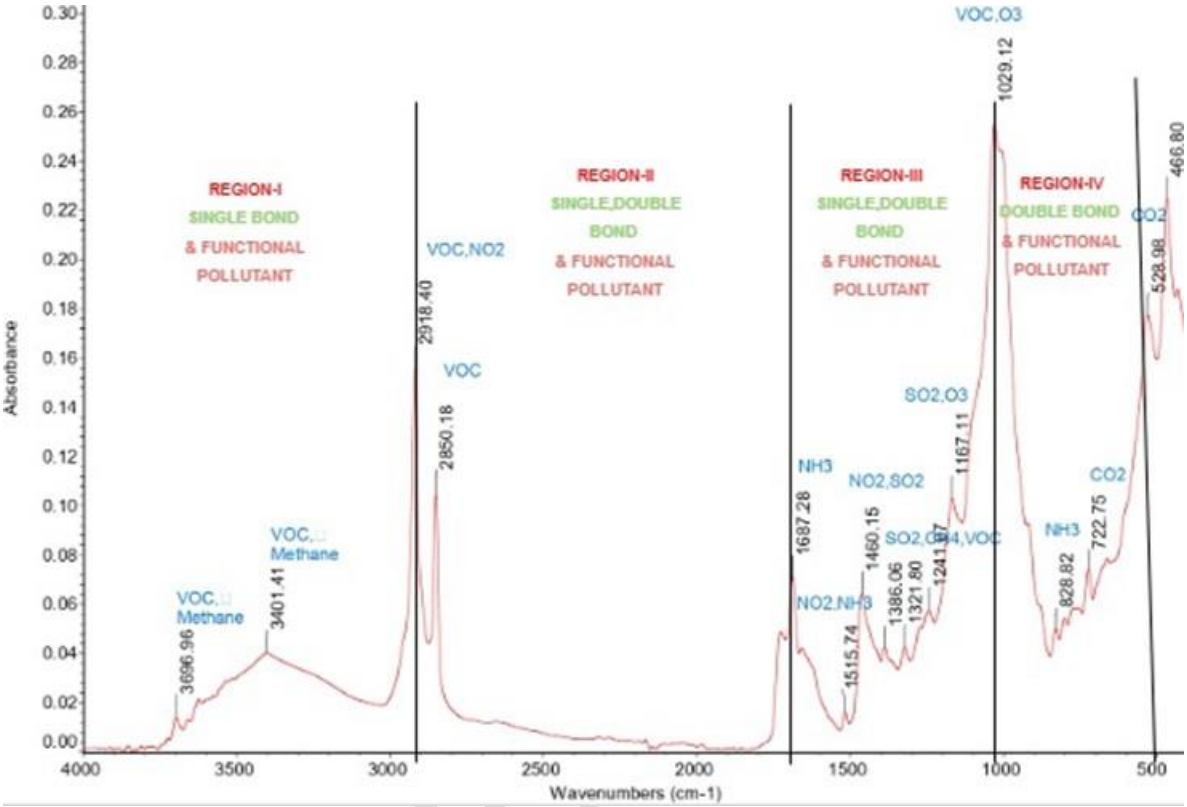

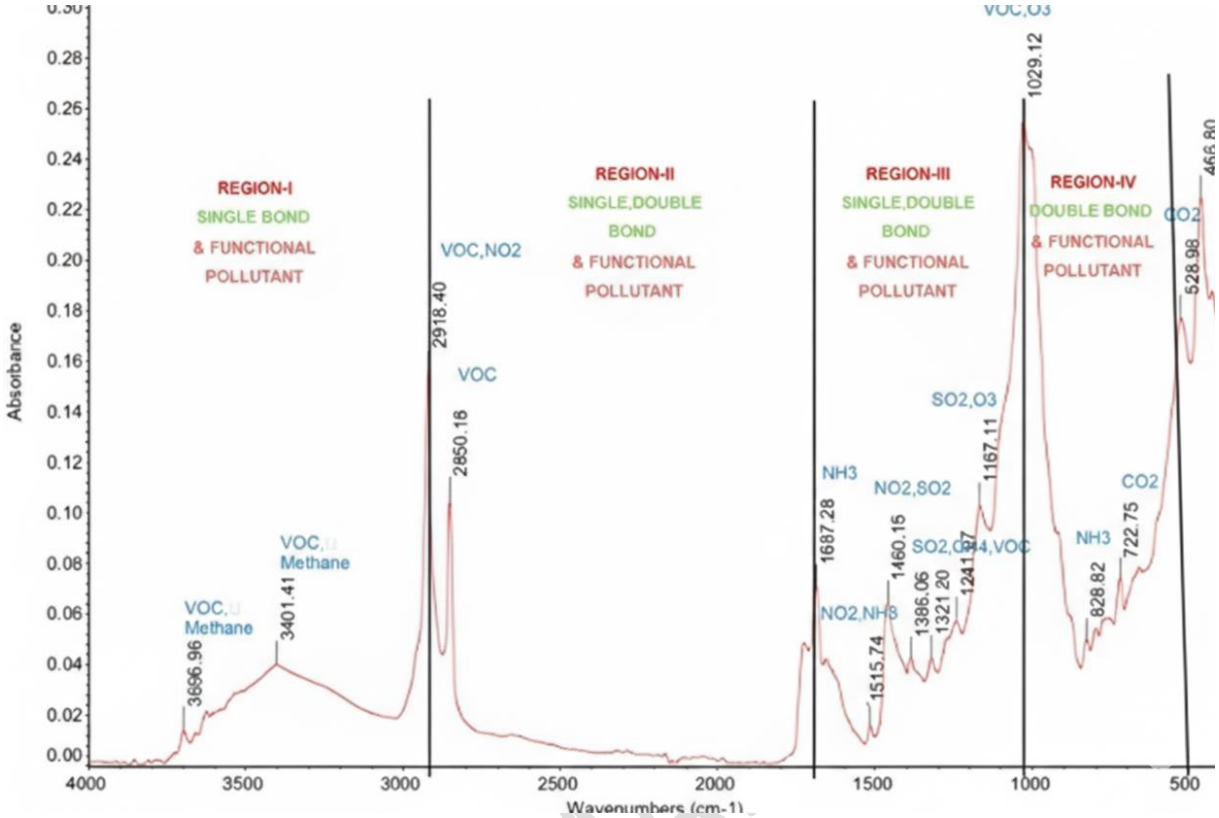

Figure 6: Pollutant spectrum of roadside tree samples from a high-traffic area

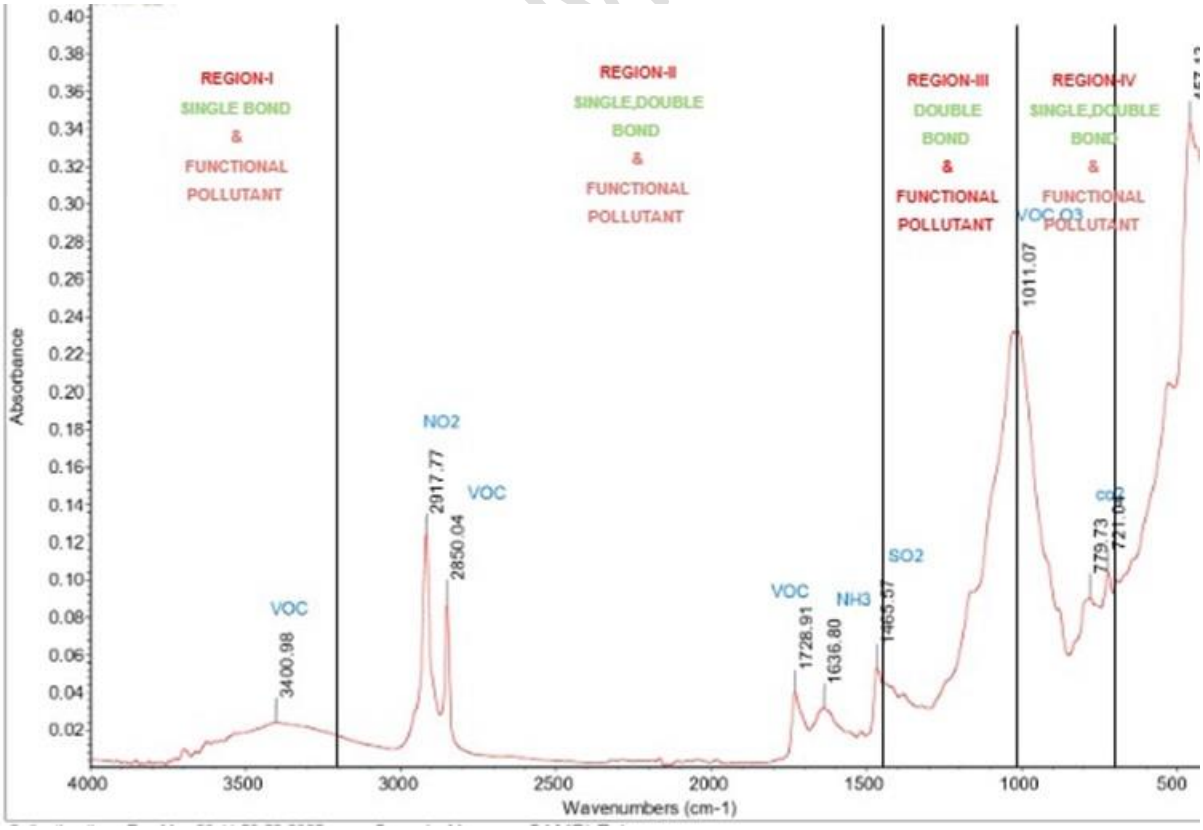

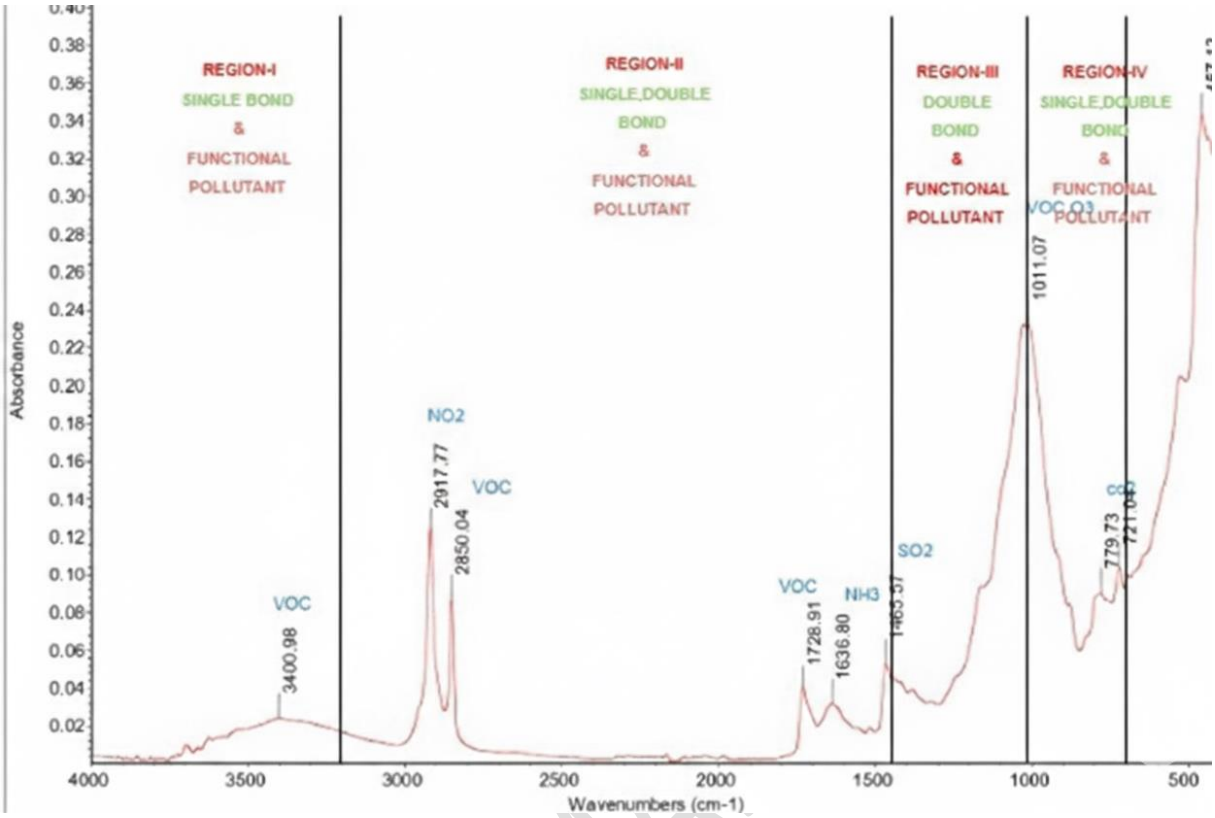

Figure 7: Pollutant spectrum of roadside tree samples from residential low-traffic area

The spectrum patterns provide the information about the sample under laboratory examination. The location and strength of certain C-H stretch characteristics of hydrocarbons depend on the extension of aromatic bonding, and they were easily identified. The majority of C-H stretching takes place in the functional group's first area, which spans 2800 to 3696 cm^{-1}. IR sulfonyl acid, C-H, and S=O are examples of cascaded stretching vibrations that can occasionally be created when the coupling connections overlap. The VOC and NH3 groups are found in the 4000–2850 cm^{-1} range. Hydrocarbon depends on the presence or absence of C-O, and C-O stretching is similar to that of ether and detect its presence. Stronger NO2 occupies 1687 cm^{-1}, medium density NO2 stretching occupies 1460 cm^{-1}, and N-O compound occupies 2918 cm^{-1}.

Method 3: Haryana Pollution Control Board - Air Quality Index Values Data Collection.
Data on environmental pollutants was obtained from the Haryana Pollution Control Board (HPCB) department. Government-established Air Quality Index (AQI) categories for each pollutant and data collected for experimental research.

4.1 AIR Pollutant Measurement with FTIR spectrometer values

The pollutant deposition from the leaf are analysed with spectrum's properties,such as shape, intensity, and bond. The peak with functional group C-H has a higher intensity at a wavelength of 3401.41 cm^{-1} and a radiation absorbance of 0.042 A. Functional group is used to identify the contaminant such as hydrocarbon. To determine the kind of pollutant from a leaf, the procedure is repeated for each peak in the spectrum. For leaf sample data from high and low traffic areas,

Tables II and III display single and double C-H bonding with varying wave numbers, such as 3696.96 cm^{-1} and 2918.4 cm^{-1}.

Table II: FTIR spectrophotometer results for dry leaf spectrum measurement in a high-traffic roadside area

High Traffic Area						
S.NO	Height in Meters(m)	Wavelength (cm^{-1})	Absorbance IR spectra	Functional Bond	Name of Polluant	Group of functional name of Pollutant
1	3.04 m	3696.96	0.03	C-H	VOC,CH4	Hydrocarbon
2	3.02 m	3401.41	0.042	C-H	VOC,CH4	Hydrocarbon
3	2.09 m	2918.4	0.16	C-H,N=O	VOC,NO2	Hydrocarbon,Nitro group
4	2.07 m	2850.18	0.13	C-H	VOC	Hydrocarbon
5	2.5 m	1687.28	0.07	N-H	NH3	Amine
6	2.4 m	1515.74	0.01	N=O,N-H	NO2,NH3	Sulfonyl,Amine
7	2.3 m	1460.15	0.05	N=O,S=O	NO2,SO2	Nitro group,Sulfonyl
8	2.1 m	1386.06	0.048	S=O,C-H	SO2,CH4,VOC	Hydrocarbon,Sulfonyl
9	2 m	1029.12	0.25	C-H,O-O	VOC,O3	Hydrocarbon,Ozonide
10	1.5 m	722.75	0.07	C=O	CO2	Carbonyl

Table III: FTIR spectrophotometer results for dry leaf spectrum measurement in a residential low-traffic roadside area

Residential Low Traffic Area						
S.NO	Height in Meters (m)	Wavelength (cm^{-1})	Absorbance IR spectra	Functional Bond	Name of Polluants	Group of functional name of Pollutant
1	3.02 m	3400.98	0.02	C-H	VOC	Hydrocarbon
2	2.9 m	2917.77	0.13	N=O	NO2	Nitro group
3	2.7 m	2850.04	0.09	C-H	VOC	Hydrocarbon
4	2.6 m	1728.1	0.03	C=O	VOC	Hydrocarbon
5	2.5 m	1636.8	0.02	N-H	NH3	Amine
6	2.3 m	1465.57	0.05	S=O	SO2	Sulfonyl
7	2 m	1011.07	0.23	C-O,O-O	VOC,O3	Hydrocarbon,Ozonide
8	1.5 m	779.73	0.08	C-O,C=O	VOC,CO2	Hydrocarbon,Carbonyl
9	1.5 m	721.04	0.09	C-O	VOC	Hydrocarbon

10	1.3 m	457.13	0.34	S=O	SO2	Sulfonyl

The functional group is sulfonyl with functional bond S=O at 1465.57 cm^{-1}, 0.05 A. For two distinct absorbance factors, hydrocarbon is visible at 1728.1 cm^{-1}, 0.03A, and 1011.07 cm^{-1}, 0.23A. Double-bond stretching vibration happens at 2918.4 cm^{-1}, 0.16A for both frequencies. Amine is found for two distinct absobance factors with a single functional bond N-H at 1687.28 cm^{-1},0.07A and 1636.8 cm^{-1},0.02A.Two hydrogen proton bond donors are found for both high roadside traffic area and low traffic area side collected leaf spectra.However, there are slight gearbox shifts. Based on the transmitted wavelength and absorbance, it is clear from the tables that there are substantially few pollutants on the side of the residential low-traffic region.

4.2 Vision Transformer algorithm analysis for air pollutants prediction from leaf image

Vision Transformer (ViT) is used interest in image classification and detection.ViT relies on transformer-based design, whereas conventional CNNs rely on convolution-based architecture. Transformer-based design increases the efficiency of image processing by gathering information from picture data patterns. ViT has the ability to automatically process visual features and use them for pattern recognition-based image categorisation and detection [37].The transformer uses an encoder and decoder to synchronise its acyclic network structure with parallel computation. Furthermore, a self-attention mechanism in transformers reduces training time and improves performance [38,39,40]. Detection accuracy and shows substantial efficacy, ViT plays a vital role in air pollutant detection on roadside tree leaves through streetwise values from leaf images acquires from smart phone as shown in figure 8 .

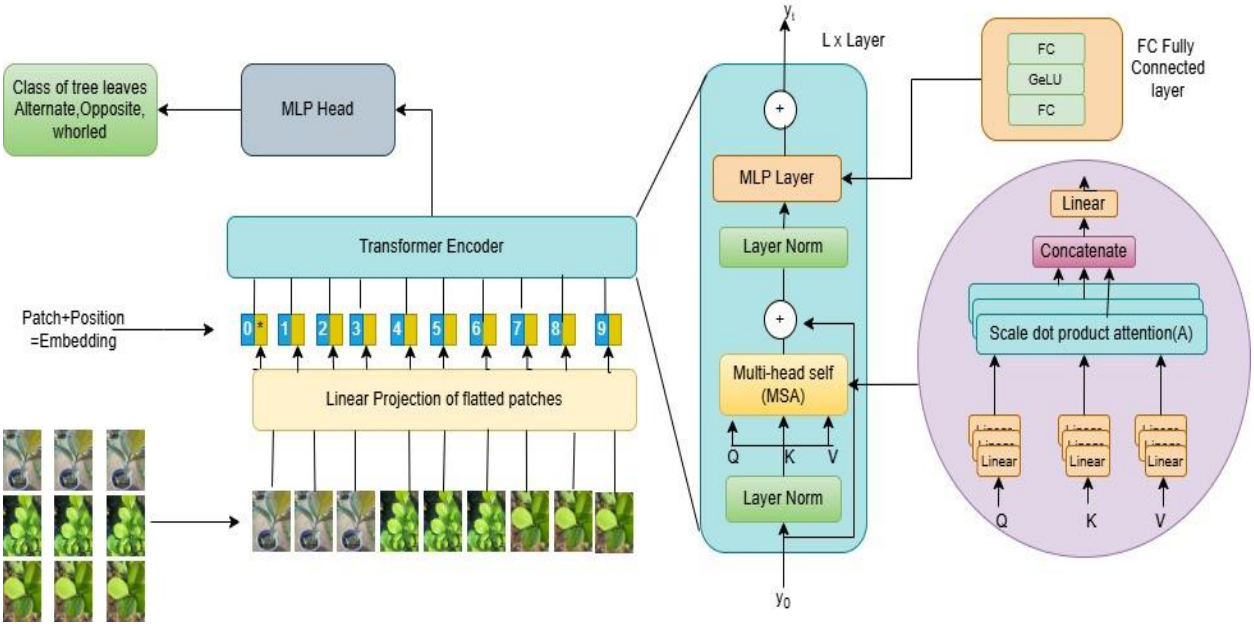

Figure 8: ViT architecture phyllotaxy based leaf type

5. Expertimental finding and performance evaluation:

This section uses a variety of metrics to evaluate the effectiveness of a machine learning-based model for air pollution prediction utilising FTIR spectrometer values, leaf images vlaues, and CPCB values.Regression analyses provide information about deposition of pollutant. To evaluate the model's capacity and estimate pollutant concentration and classify air quality levels as shown in screenshot 1.The performance evaluation metrics are evaluated.

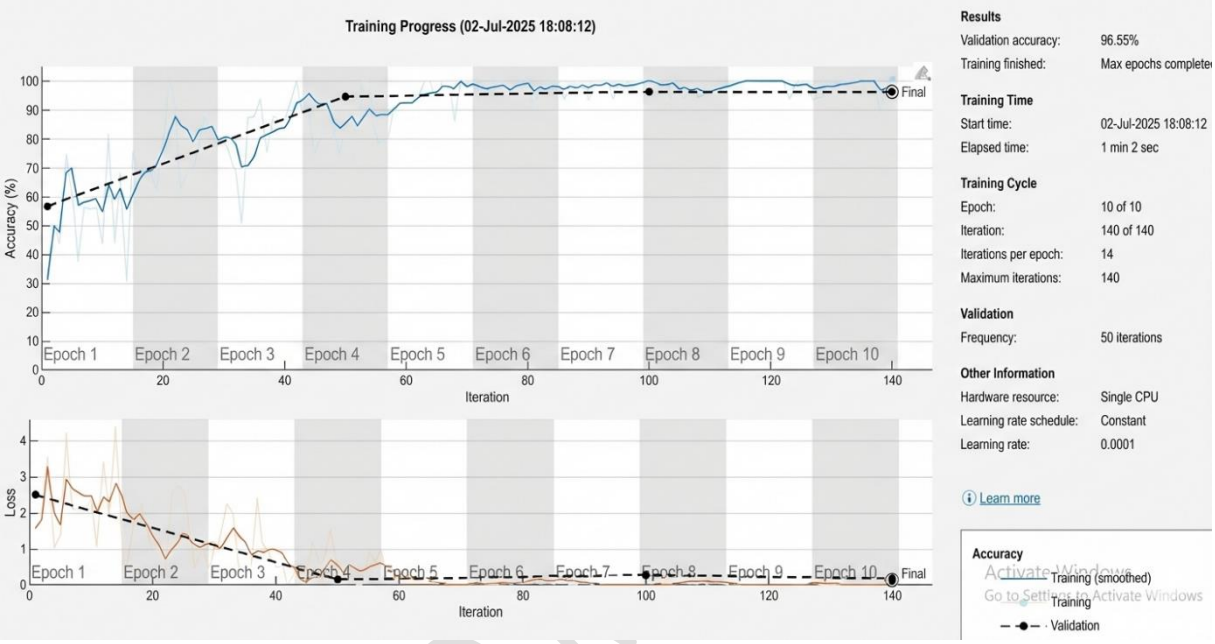

screenshot 1: Accuracy for the leaf image of Alternate, Opposite and Whorled type

The test and validation of the leaf dataset for the three classes of alternate, opposite, and whorled leaves are displayed in screenshot 2 of output screen . On the test set, the model provides flawless classification, with no classification errors for any of the three types of leaf datasets. A perfect accuracy rate of 100% was attained by the categorisation model. According to the validation result, the alternate leaf has a predicted value of 1.00, the opposite leaf has a prediction of.94, and the whorled leaf has a prediction of.95. These results indicate variability, which causes overlapping morphological or spectral properties in the leaf photos taken at

different pollution levels.

Command Window

```
--- VALIDATION RESULTS ---
Classification Metrics:
          Class            Precision    Recall     F1_Score
    ___________________    _________    _______    ________

    {'Alternate leaf'}           1           1          1
    {'Opposite leaf' }     0.94444     0.94444    0.94444
    {'Whorled leaf'  }        0.95        0.95       0.95

--- TEST RESULTS ---
          Class            Precision    Recall     F1_Score
    ___________________    _________    ______     ________

    {'Alternate leaf'}           1           1          1
    {'Opposite leaf' }           1           1          1
    {'Whorled leaf'  }           1           1          1
```

Screenshot 2: Shows test and validation of leaf dataset of three classes

5.1 **Classification metric and result:**

5.1.1 **Accuracy**

The performance of a detection model is determined by accuracy. Accuracy is calculated using the formula below shown in equation(1):

$$\text{Accuracy}= \frac{TP+TN}{TP+FP+TN+FN} \quad (1)$$

5.1.2 Precision

Precision is the ratio of true positives to all positive values as shown in equation (2). This measure is useful, when false positives are taken into account in references.

$$\text{Precision}= \frac{TP}{TP+FP} \quad (2)$$

5.1.3 Recall

In recall positive and false negative data are added and determined the ratio of real positives as shown in equation(3).

$$\text{Recall}= \frac{TP}{TP+FN} \quad (3)$$

5.1.4 F1-Score

The F1-score evaluates detection accuracy by combining precision and recall. It is calculated using the precision and recall harmonic means. In terms of precision and recall, which are equal,

it attains the maximum value. The following is the formula for the F1 score as shown in equation (4):

$$\text{F1-Score}=2 * \frac{Precision*Recall}{Precision+Recall} \quad (4)$$

5.1.5 Confusion matrix

Screenshot 3 illustrate the confusion matrix for validation and testing for the image has derived from the test dataset of leaf image based on phyllotaxy .The dataset has three classes of leaf image such as alternate leaf, Opposite type leaf and Whorled leaf as shown in table and figure .The metrics were computed for each class using a confusion matrix as shown in figure 10 and the accuracy is 96% as shown in figure 8.

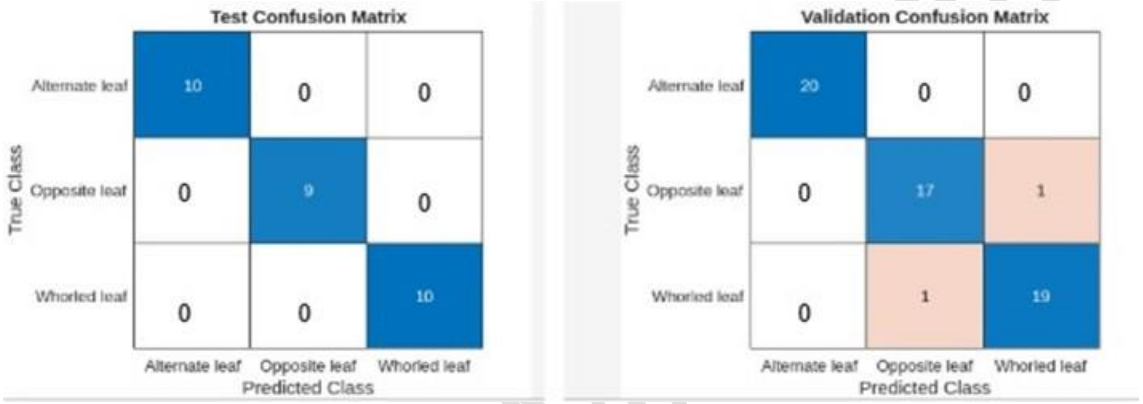

Screenshot 3: The confusion matrix for testing and validation for the leaf image of Alternate, Opposite and Whorled type

5.2 Baysian Optimized Multilevel Regression (BO-MLR) analysis for prediction of pollutant prediction :

The BO-MLR predict the real pollutant concentrations, such as PM_2, PM10, NO_2, CO, and O3 values, and assessed in addition to classification. The evaluation metrics are the coefficient of determination (R2) and the Root Mean Square Error (RMSE).Tables IV and V shows the pollutant level for residential low traffic side and roadside heavy traffic. To forecast air pollution on roadside high traffic areas and residential low traffic areas, for PM2.5, PM10, NO2, CO, and O3 are performed using the table below.

Table IV: Sample data of Air Pollutant levels obtained from CPCB station IMT Manesar, FTIR absobance and High traffic roadside leaf image

Date	Evening Timing	High traffic roadside leaf values			Pollutant Values of CPCB of IMT Manesar					FTIR Absorbance
		Contrast	Entropy	Standard Deviation	PM2.5	PM10	NO2	CO	O3	

1/3/2025	5:00 P.M	183	185	187	205	141	24	33	10	0.281
2/3/2025	5:00 P.M	190	191	189	287	198	24	54	10	0.283
3/3/2025	5:00 P.M	234	237	239	365	313	30	43	10	0.285
4/3/2025	5:00 P.M	230	235	231	330	315	26	32	17	0.286
5/3/2025	5:00 P.M	196	194	192	292	224	19	45	11	0.289
6/3/2025	5:00 P.M	230	234	237	345	345	28	64	11	0.293
7/3/2025	5:00 P.M	279	281	277	333	239	20	46	10	0.297
8/3/2025	5:00 P.M	297	289	295	318	241	21	50	10	0.301
9/3/2025	5:00 P.M	314	291	297	392	335	29	108	11	0.305
10/3/2025	5:00 P.M	306	294	299	371	410	24	62	11	0.309
11/3/2025	5:00 P.M	276	274	283	301	215	24	46	10	0.314
12/3/2025	5:00 P.M	295	293	287	322	245	23	51	11	0.317
13/3/2025	5:00 P.M	299	297	291	325	232	22	55	10	0.32
14/3/2025	5:00 P.M	279	274	271	297	206	23	31	10	0.323
15/3/2025	5:00 P.M	95	78	98	114	119	25	18	11	0.326
16/3/2025	5:00 P.M	192	189	198	200	172	28	31	11	0.327
17/3/2025	5:00 P.M	226	242	245	262	221	27	32	11	0.329
18/3/2025	5:00 P.M	224	222	226	273	234	28	40	10	0.33
19/3/2025	5:00 P.M	282	299	297	330	292	33	45	11	0.33
20/3/2025	5:00 P.M	178	166	196	208	202	30	20	11	0.33
21/3/2025	5:00 P.M	177	189	198	260	222	16	48	11	0.33
22/3/2025	5:00 P.M	274	280	289	350	338	9	61	10	0.33
23/3/2025	5:00 P.M	271	292	282	296	238	8	39	22	0.331
24/3/2025	5:00 P.M	233	213	217	237	214	8	28	5	0.332
25/3/2025	5:00 P.M	139	136	139	184	155	6	38	6	0.333
26/3/2025	5:00 P.M	244	248	274	308	193	6	29	5	0.335

27/3/2025	5:00 P.M	149	145	148	206	143	7	22	5	0.337
28/3/2025	5:00 P.M	138	136	133	142	149	8	26	10	0.339
29/3/2025	5:00 P.M	151	151	151	290	237	7	47	10	0.341
30/3/2025	5:00 P.M	180	173	173	139	111	6	18	11	0.342

As presented in figure 9 shows the analysis of the five pollutants actual and predicted value in roadside high traffic area.

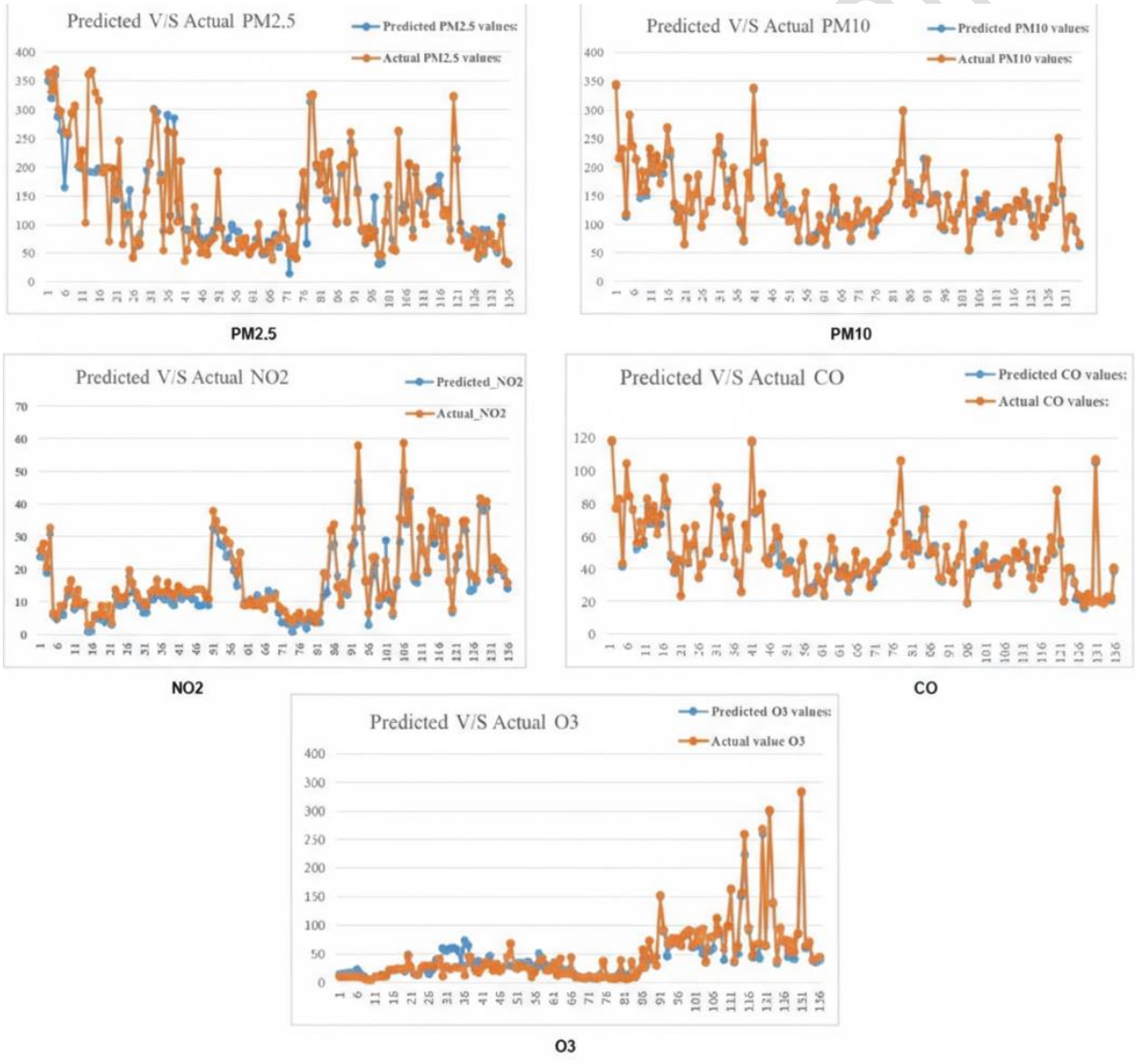

Figure 9:The variation analysis of the five pollutants in actual and predicted value in roadside high traffic area are shown.

The MATLAB code was executed, and the concentrations of the five pollutants were determined.Figure 10 shows the model's performance in predicting air contaminants. demonstrates the variance in the amounts of PM2.5, PM10, NO2, CO, and O3 pollutants and shows a remarkable R2 performance value.

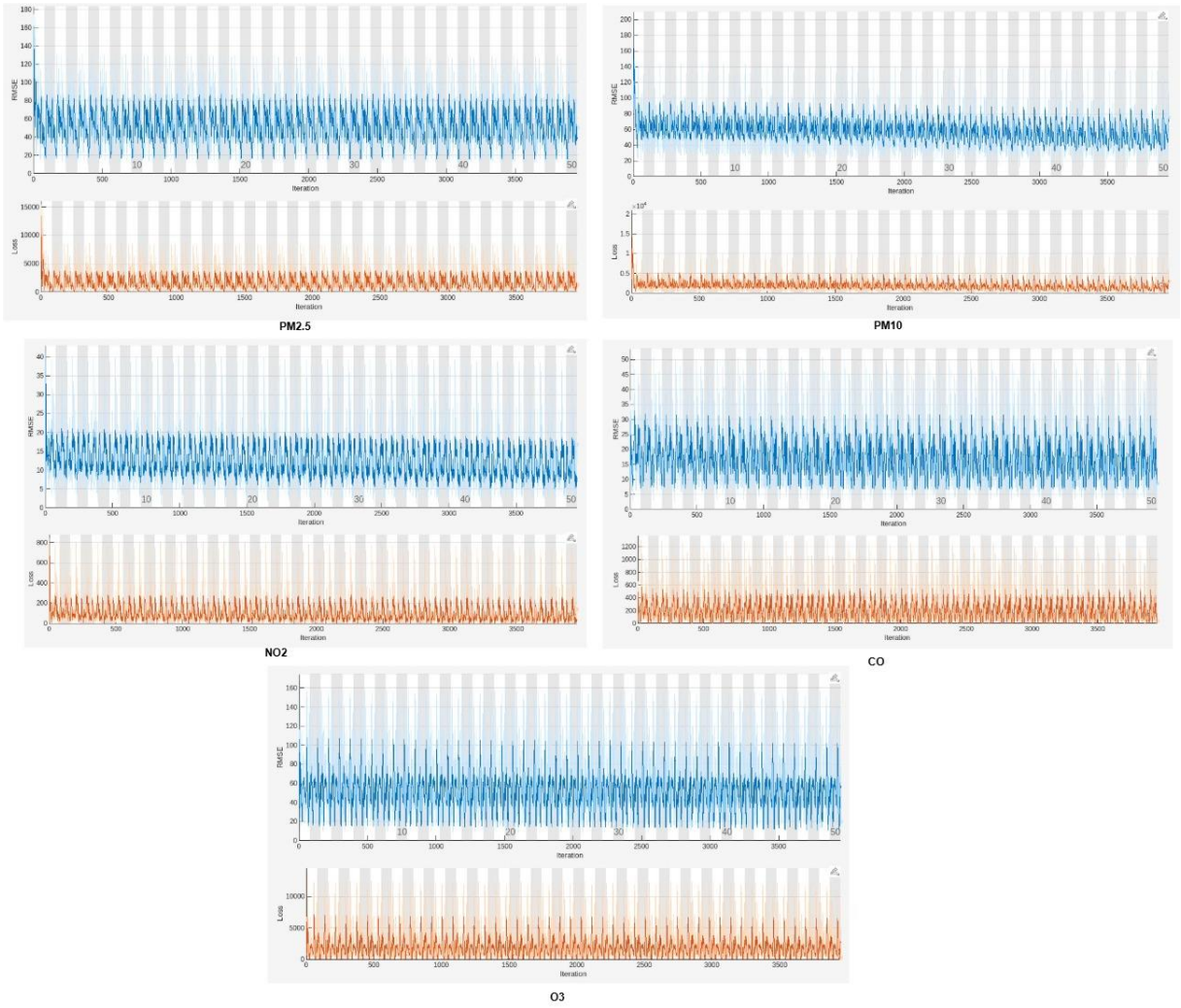

Figure 10: The performance variation of R2 scores and RMSE for five pollutants in roadside high traffic area.

Predicted and Actual value of Pollutants roadside High traffic area									
Predicted PM2.5 values:	Actual PM2.5 values:	Predicted PM10 values:	Actual PM10 values:	Predicted NO2 values:	Actual NO2 values:	Predicted CO values:	Actual CO values:	Predicted O3 values:	Actual O3 values:
351	365	342	345	24	26	31	32	14	10
320	333	214	215	25	28	61	64	15	10
361	371	231	232	19	21	40	50	16	11
289	301	114	119	31	33	42	45	18	10
265	297	291	292	6	7	43	47	14	11
218	262	236	238	5	6	22	26	23	10
255	260	212	214	7	9	21	24	15	11
294	296	145	155	6	9	41	30	10	6
305	308	193	193	12	14	36	30	4	5
201	204	150	158	16	17	37	33	4	5
RMSE: 5.7		RMSE: 9.4		RMSE: 4.1		RMSE: 6.6		RMSE: 0.4	
R^2 Score: 0.93		R^2 Score: 0.88		R^2 Score: 0.92		R^2 Score: 0.89		R^2 Score: 0.92	
Predicted PM2.5 (New Leaf): 230.02		Predicted PM10 (New Leaf): 185.16		Predicted NO2 (New Leaf): 18.89		Predicted CO (New Leaf): 38.68		Predicted O3 (New Leaf): 43.25	

Screenshot 4: Results of the **Phyllo-ViT model** for AQI prediction in roadside high traffic area.

Results from the Phyllo-ViT machine learning model used to forecast air quality are shown in screenshot 4 of output screen that show which will be next predicted value of pollutants with the new leaf, along with performance indicators (R2, RMSE). The data show that the models generally achieve higher accuracy for PM2.5 pollution, producing an R2 score of 0.93 and an RMSE of 5.7 in high-traffic areas along the roadside. They also predicted new leaf values, such as 230.3.With a predicted new leaf value of 185.16, the PM10 pollutant had the lowest accuracy, yielding an R2 score of 0.88 and an RMSE of 9.4.Table V shows about the dataset used for residential low traffic roadside leaf values.In this table Air pollutant values obtained from CPCB station Sector-82,gurugram,FTIR absorbance values,and Residential low traffic roadside leaf image value.

Table V: Air Pollutant levels obtained from CPCB station Sector-82,Gurugram, FTIR absobance and Residential Low traffic roadside leaf image

Dates	Evening Timing	Residential Low traffic roadside leaf values			Pollutant Values of CPCB of Sector-82, Gurugram					FTIR Absorbance
		Contrast	Entropy	Standard Deviation	PM2.5	PM10	NO2	CO	O3	
1/3/2025	5:00 P.M	215	212	209	205	141	24	33	10	0.159
2/3/2025	5:00 P.M	214	211	209	287	198	24	54	10	0.16
3/3/2025	5:00 P.M	215	212	210	365	313	30	43	10	0.162
4/3/2025	5:00 P.M	215	213	211	330	315	26	32	17	0.164

5/3/2025	5:00 P.M	216	214	210	292	224	19	45	11	0.169
6/3/2025	5:00 P.M	216	214	211	345	345	28	64	11	0.172
7/3/2025	5:00 P.M	214	214	213	333	239	20	46	10	0.173
8/3/2025	5:00 P.M	215	217	216	318	241	21	50	10	0.175
9/3/2025	5:00 P.M	218	219	219	392	335	29	108	11	0.177
10/3/2025	5:00 P.M	187	187	186	371	410	24	62	11	0.178
11/3/2025	5:00 P.M	184	183	183	301	215	24	46	10	0.179
12/3/2025	5:00 P.M	181	180	180	322	245	23	51	11	0.18
13/3/2025	5:00 P.M	180	180	180	325	232	22	55	10	0.182
14/3/2025	5:00 P.M	180	181	182	297	206	23	31	10	0.184
15/3/2025	5:00 P.M	181	184	185	114	119	25	18	11	0.186
16/3/2025	5:00 P.M	183	186	187	200	172	28	31	11	0.187
17/3/2025	5:00 P.M	191	193	193	262	221	27	32	11	0.188
18/3/2025	5:00 P.M	191	193	193	273	234	28	40	10	0.188
19/3/2025	5:00 P.M	174	172	174	330	292	33	45	11	0.187
20/3/2025	5:00 P.M	141	140	146	208	202	30	20	11	0.186
21/3/2025	5:00 P.M	204	202	197	260	222	16	48	11	0.185
22/3/2025	5:00 P.M	204	201	196	350	338	9	61	10	0.185
23/3/2025	5:00 P.M	205	202	197	296	238	8	39	22	0.185
24/3/2025	5:00 P.M	208	203	198	237	214	8	28	5	0.186
25/3/2025	5:00 P.M	207	202	198	184	155	6	38	6	0.188
26/3/2025	5:00 P.M	206	204	199	308	193	6	29	5	0.19
27/3/2025	5:00 P.M	209	206	200	206	143	7	22	5	0.192
28/3/2025	5:00 P.M	212	209	203	142	149	8	26	10	0.196
29/3/2025	5:00 P.M	215	213	208	290	237	7	47	10	0.199

30/3/2025	5:00 P.M	184	184	184	139	111	6	18	11	0.204

As presented in figure 11 the analysis of the five pollutants in actual and predicted value in roadside residential low traffic area.

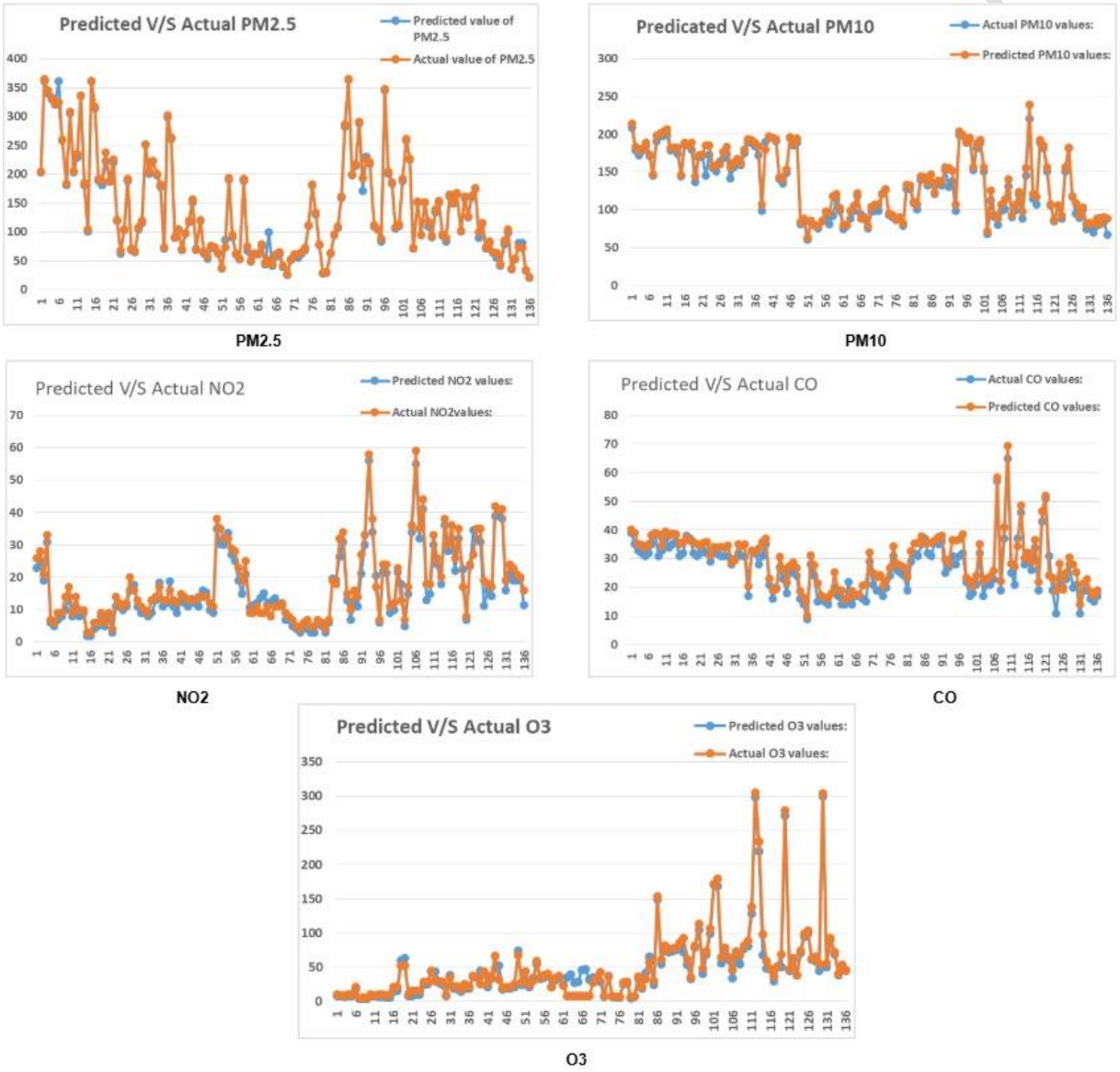

Figure 11: The variation analysis of the five pollutants in actual and predicted value in a residential low traffic area are shown.

The analysis of the data showed that the model performed better in predicting air pollutants in residential low traffic areas.The performance variance of R2 scores and RMSE for five contaminants in a roadside low- traffic area is displayed in figure 12.

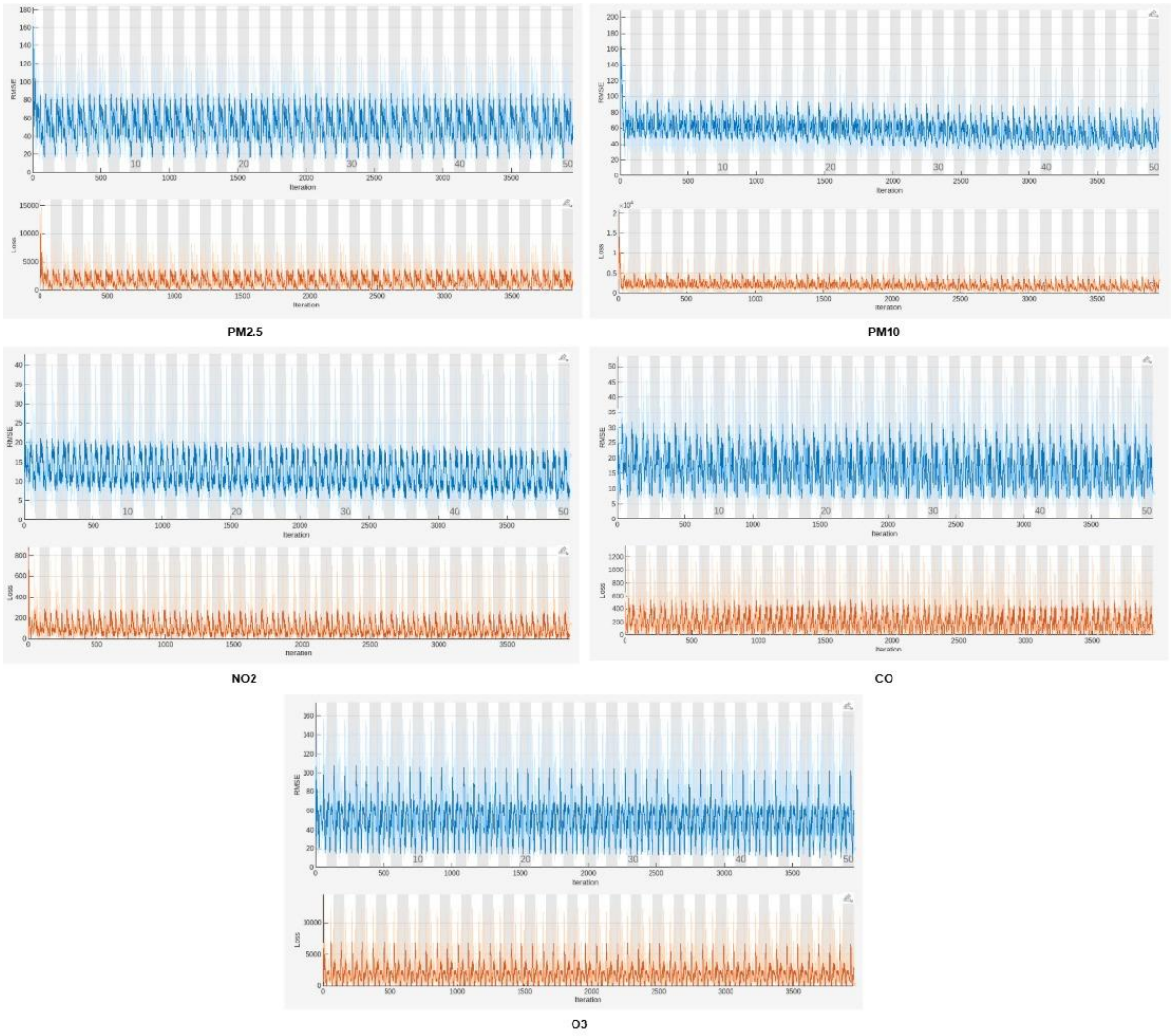

Figure 12: The performance variation of R2 scores and RMSE for five pollutants in roadside high traffic area.

The data indicate that, in general, the models achieve higher accuracy for NO2 pollutant in which it produced an R2 score of 0.96, and an RMSE of 3.7 in roadside residential low traffic area also predicted the new leaf value such as 18.40 as show in screenshot 5 .The lowest accuracy for PM10 pollutant in which it produced R2 score of 0.93, and an RMSE of 7.3 with predicted the new leaf value such as 170.80.

Predicted and Actual value of Pollutants roadside residential low traffic area									
Predicted PM2.5 values:	Actual PM2.5 values:	Predicted PM10 values:	Actual PM10 values:	Predicted NO2 values:	Actual NO2 values:	Predicted CO values:	Actual CO values:	Predicted O3 values:	Actual O3 values:
203	205	208	213	23	26	39	40	9	11
361	365	179	184	25	28	35	39	8	10
341	345	172	178	19	21	33	35	7	10
331	333	179	181	31	33	32	35	9	11
321	322	185	189	6	7	31	34	9	11
361	325	171	173	5	6	32	35	18	22
259	260	145	147	7	9	35	38	4	5
181	184	191	198	8	9	39	39	4	6
306	308	197	201	10	14	31	39	4	5
203	206	198	204	14	17	37	33	9	11
RMSE: 4.4		RMSE: 7.3		RMSE: 3.7		RMSE:5.2		RMSE: 0.27	
R^2 Score: 0.95		R^2 Score: 0.93		R^2 Score: 0.96		R^2 Score: 0.94		R^2 Score: 0.95	
Predicted PM2.5 (New Leaf): 230.02		Predicted PM10 (New Leaf): 170.80		Predicted NO2 (New Leaf): 18.40		Predicted CO (New Leaf): 30.06		Predicted O3 (New Leaf): 42.70	

Screenshot 5: Results of **Phyllo-ViT model** for AQI prediction in roadside residential low traffic area.

6. Discussion

According to the results shown in screenshot 4 and 5 in this study, the suggested model's performance metrics are significantly superior.The model recoded an R2 value 0.96 in roadside residential low traffic area. Similarly, in predicting other pollutants such as PM2.5,NO2,CO,and O3 levels ,the model recorded an R2 value.Its strong predictive ability in environmental monitoring is further demonstrated.

Overall, the Phyllo-ViT model has shown encouraging performance when applied to a task of forecasting air contaminants from a tree leaf image. After extensive testing and improvement, this model has demonstrated a remarkable ability to correctly classify a variety of air contaminants, however with considerable variances in efficacy throughout types.In addition to highlighting machine learning's potential for environmental monitoring, the analysis's results also point out areas that require development, particularly in the prediction of other pollutants. However, the dataset is limited to a specific urban area, and it has not been validated across a wider range of geographical regions. Future research using larger and more diverse data sets may improve the methodology's generalisability even more.

The study's limitations include the fact that Tree species, leaf age, seasonal fluctuations, and local meteorological conditions—all of which are not consistently controlled across all sampling locations—all affect how accurately pollutants are predicted. Inconsistencies or missing data from AQI monitoring stations (HPCB) could affect forecasting reliability and prediction accuracy since the integrated framework depends on the availability and temporal alignment of diverse data sources.Phyllo-ViT model accuracy of pollutant PM2.5 $R^2 = 0.96$

(residential low traffic), PM2.5 $R^2 = 0.93$ (high traffic); RMSE values for PM2.5 were 3.7 and 5.7 respectively.

Future studies will concentrate on using lightweight Vision Transformer (ViT) models tailored for edge devices and portable spectrometers to enable real-time deployment.To increase the reliability and scalability of the suggested methodology, cross-seasonal and cross-city validation will be carried out utilizing bigger and more varied datasets. In order to provide ongoing, street-level AQI monitoring for smart city applications, the system will also be connected with IoT infrastructure and municipal dashboards.

7. Conclusion

In this work, an innovative methodology to predicting air pollutants from streetwise roadside tree leaves is presented. AQI pollutants are measured in area-wise and not street-wise. Measurements must be made of the amount of traffic and the amount of pollutants deposited in the AQI area. There is no measurement of AQI on the roads. The study's conclusions are crucial because they provide fresh perspectives on forecasting air quality street-wise. The study's findings allow for the following conclusions:

1. By combining techniques I and III—which make use of FTIR values, CPCB values, and streetwise outdoor plant leaf images based on Phyllotaxy—this work offers a novel way to predict air contaminants.
2. The suggested Phyllo-ViT model handles tabular FTIR and CPCB data by utilising the Vision Transformer architecture to efficiently build complicated representations from leaf imagery, bolstered by conventional machine learning approaches.
3. In a roadside low traffic region, the model's coefficient of determination (R2) of 0.96 indicates high agreement between predicted and actual air pollution levels, demonstrating its strong predictive performance.
4. The use of vegetation (FTIR data and leaf images) as a bioindicator has considerable promise for low-cost, non-invasive environmental monitoring, particularly in urban or semi-urban regions without extensive monitoring networks.
5. Future research can investigate new plant species or spectrum characteristics, real-time deployment, and wider geographic generalisation. ViT+CNN hybrids and attention-enhanced fusion layers are two examples of deep learning variations that may also enhance performance.

Declaration

Ethical Approval

Not Applicable,This is an observational study conducted on tree leaves, with no involvement of human participants or animals. The Departmental Research Ethics Committee has reviewed the study and confirmed that formal ethical approval is not required.

Consent to Participate

Not applicable, as the study involved no human participants.

Consent to Publish
All authors have read and approved the final manuscript and consent to its submission and potential publication.
Data Availability Statement
The data supporting the findings of this study are included within the article. Additional data used in this research are publicly available at the Central Pollution Control Board's Air Quality portal: https://airquality.cpcb.gov.in/AQI_India/.
Author Contributions
Neelam Yadav: Conceptualization, methodology, writing – original draft.
Sunil K. Singh: Formal analysis, supervision, writing – review & editing.
Dinesh Sharma: Data interpretation, data curation, validation & analysis, supervision.
Funding
The authors declare that no funds, grants, or other financial support were received during the preparation of this manuscript.
Competing Interests
The authors have no relevant financial or non-financial interests to disclose.

References

[1] World Health Organization. (2023). Air Pollution. https://www.who.int/news-room/fact-sheets/detail/ambient-(outdoor)-air-quality-and-health

[2] Escobedo FJ, Wagner JE, Nowak DJ (2008) Analyzing the cost effectiveness of Santiago, Chile's policy of using urban forest to improve air quality. J Environ Manag 86:148–157

[3] Varshney CK (1985) Role of plant in indicating, monitoring and mitigating air pollution. In: Air pollution and plants: a state of the art report (Eds. G.V. Subrahmanium, D.N. Rao, C.K. Varshney and D.K. Viswas.). Ministry of Environment and Forest, New Delhi 146–170

[4] Pradhan AA, Pattanayak SK, Bhadra AK, Ekka K (2016) Air pol lution tolerance index of three species along national high way—6 between Ainthapali to Remed, Sambalpur District, Western Odisha, India. Biolife 4(1):111–120

[5] Banerjee S, Banerjee A, Palit D (2022) Morphological and biochemi cal study of plant species- a quick tool for assessing the impact of air pollution. J Clean Prod 339:130647. https:// doi. org/ 10. 1016/j. jclepro.2022.130647

[6] Wróblewska K, Jeong BR (2021) Effectiveness of plants and green infrastructure utilization in ambient particulate matter removal. Environ Sci Eur 33:110. https:// doi. org/ 10. 1186/ s12302-021-00547-2

[7] Sahu C, Sahu SK (2015) Air pollution tolerance index (APTI), anticipated performance index (API), carbon sequestration and dust collection potential of Indian tree species—A review. Int J Emerg Res Manag Technol 4(11):37–40

[8] Chaturvedi RK, Prasad S, Rana S, Obaidullah SM, Pandey V & Singh H (2013) Effect of dust load on the leaf attributes of the tree species growing along the roadside. Environmental Monitoring and Assessment 185(1): 383–391.

[9] Smith, T. E. L., Wooster, M. J., Tattaris, M., and Griffith, D. W. T.: Absolute accuracy and sensitivity analysis of OP-FTIR retrievals of CO2, CH4 and CO over concentrations representative of "clean air" and "polluted plumes", Atmos. Meas. Tech., 4, 97–116, https://doi.org/10.5194/amt-4-97-2011, 2011.

[10] Liu N., Karunakaran C., Lahlali R., Warkentin T., Bueckert R.A. 2019. Genotypic and heat stress effects on leaf cuticles of field pea using ATR-FTIR spectroscopy. Planta 249(2): 601–613.

[11] Bharti SK, Trivedi A, Kumar K (2017) Air pollution tolerance index of plants growing near an industrial site. Urban Clim. https ://doi. org/10.1016/j.uclim.2017

[12] Nithamathi, C. P., and Indira, V., 2005, Impact of air pollution On Ceasalpinia sepiaria Linn. in Tuticorin City., Indian Journal of Environment and Ecoplanning, 10 (1), 449–452.

[13] Steubing, L., Fangmier, A., and Both, R., 1989, Effects of SO2, NO2, and O3 on Population Development and Morphological and Physiological parameters of Native Herb Layer Species in a Beech Forest., Environmental pollution, 58(4), 281-302.

[14] Nuhoglu, Y., 2005, The harmful effects of air pollutants around the Yenikoy thermal power plant on architecture of Calabarian pine (Pinus brutila Ten.) needles., Journal of Environmental Biology, 26(2), 315–322.

[15] Pravin U. Singare, Madhumita S. Talpade, Physiological Responses of Some Plant Species as a Bio-Indicator of Roadside Automobile Pollution Stress Using the Air Pollution Tolerance Index Approach, International Journal of Plant Research, Vol. 3 No. 2, 2013, pp. 9-16. doi: 10.5923/j.plant.20130302.01.

[16] Zhang, H.; Zhang, Y.; Wang, Z.; Ding, M.; Jiang, Y.; Xie, Z. Traffic-related metal (loid) status and uptake by dominant plants growing naturally in roadside soils in the Tibetan plateau, China. Sci. Total Environ. 2016, 573, 915–923. [CrossRef]

[17] Rai, K. Biodiversity of roadside plants and their response to air pollution in an Indo-Burma hotspot region: Implications for urban ecosystem restoration. J. Asia-Pac. Biodivers. 2016, 9, 47–55. [CrossRef]

[18] Majumdar, D. & Biswas, Bratisha & Majumdar, Dipanjali & Ray, Rupam. (2021). Size-Segregated Elemental Profile and Associated Heath Risk Assessment of Road Dust along Major Traffic Corridors in Kolkata Mega City. Atmosphere. 12. 1677. 10.3390/atmos12121677.

[19] Wen, L., Yuan, Y., Zeng, H., & Ma, S. (2026). The Impact of ESG Performance on Textile Industry Green exports under the Dual Carbon Goals. Global NEST Journal. https://doi.org/10.30955/gnj.07977

[20] Zhang, G., Ma, S., Zheng, M., Li, C., Chang, F. and Zhang, F., 2025. Impact of digitization and artificial intelligence on carbon emissions considering variable interaction and heterogeneity: An interpretable deep learning modeling framework. Sustainable Cities and Society, 125, p.106333.

[21] Wang, Z., Wang, F., and Ma, S. (2025). Research on the Coupled and Coordinated Relationship Between Ecological Environment and Economic Development in China and its Evolution in Time and Space. Polish Journal of Environmental Studies, 34(3), pp.3333–3342. https://doi.org/10.15244/pjoes/188854Seinfeld, J. H. (1975). Air pollution: physical and chemical properties. McGraw Hill, U. S. A.

[22] Seinfeld, J. H. (1975). Air pollution: physical and chemical properties. McGraw Hill, U. S. A.

[23] Doyle, G.J.; Tuazon, E.C.; Graham, R.A.; Mischke, T.M.; Winer, A.M.; Pitts, J.N. Simultaneous Concentrations of Ammonia and Nitric Acid in a Polluted Atmosphere and Their Equilibrium Relationship to Particulate Ammonium Nitrate. Environ. Sci. Technol. 1979, 13, 1416–1419. [CrossRef]

[24] Tuazon, E.C.; Winer, A.M.; Pitts, J.N. Trace Pollutant Concentrations in a Multiday Smog Episode in the California South Coast Air Basin by Long Path Length Fourier Transform Infrared Spectroscopy. Environ. Sci. Technol. 1981, 15, 1232–1237. [CrossRef] [PubMed]

[25] Q. Liu, S.Wang, Z. Luo, and K. Cen, “Catalysis mechanism study of potassium salts on cellulose pyrolysis by using TGA-FTIR analysis,” Journal of Chemical Engineering of Japan, vol. 41, no. 12, pp. 1133–1142, 2008.

[26] Lahlali R, Jiang Y, Kumar S, Karunakaran C, Liu X, Borondics F, Hallin E, Bueckert R (2014) ATR–FTIR spectroscopy reveals involvement of lipids and proteins of intact pea pollen grains to heat stress tolerance. Front Plant Sci. https://doi.org/10.3389/ fpls.2014.00747

[27] Bradley, K.S.; Brooks, K.B.; Hubbard, L.K.; Popp, P.J.; Stedman, D.H. Motor Vehicle Fleet Emissions by OP-FTIR. Environ. Sci. Technol. 2000, 34, 897–899.

[28] Tırınk S (2025) Machine learningbased forecasting of air quality index under long-term nvironmental patterns: A comparative approach with XGBoost,LightGBM, and SVM. PLoS One 20(10):e0334252. https://doi.org/10.1371/journal.pone.0334252.

[29] Lingjuan Tian1, Caihua Zhang1*, Xue Lei2(2025),Digital Economy's Role in Environmental Sustainability: Air Quality Enhancement through the 'Broadband China' Initiative.Pol. J. Environ. Stud. Vol. 34, No. 6 (2025), 7411-7421.DOI: 10.15244/pjoes/193135.

[30] Mohandas, Prajul & P, Subramanian & .R, Surendran. (2025). Deep Feedforward Air Pollution Classification Empowered by Sophia-G Optimization. 1696-1702. 10.1109/ICIMIA67127.2025.11200570.

[31] Mohandas, Prajul & P, Subramanian & R, Surendran. (2025). Optimizing Air Pollution Prediction in Urban Environments using a Hybrid RNN-PBO Model with IoT Data. 480-487. 10.1109/ICVADV63329.2025.10961386.

[32] Chaoyang Wang1, Huifang Liu2* and Shenglin Ma3(2024),Analysis of the effect of digital financial inclusion on agricultural carbon emissions in China.Global NEST Journal, Vol 26, No 8, 06313.https://doi.org/10.30955/gnj.06313.

[33] Liqin Wen1, Shenglin Ma1 and Yang Su*(2024),Analysis of the interactive effects of new urbanization and agricultural carbon emission efficiency.Global NEST Journal, Vol 26, No 4, 05927.https://doi.org/10.30955/gnj.005927

[34] Nathvani R, D V, Clark SN, Alli AS, Muller E. Beyond here and now: Evaluating pollution estimation across space and time from street view images with deep learning. Sci Total Environ. 2023 Dec 10;903:166168. doi: 10.1016/j.scitotenv.2023.166168.

[35] Suel, E., Sorek-Hamer, M., Moise, I. (2022). What You See Is What You Breathe? Estimating Air Pollution Spatial Variation Using Street-Level Imagery. Remote Sensing, 14(14), 3429. https://doi.org/10.3390/rs14143429

[36] Feldman A, Kendler S, Marshall J, . Urban Air-Quality Estimation Using Visual Cues and a Deep Convolutional Neural Network in Bengaluru (Bangalore), India. Environ Sci Technol. 2024 Jan 9;58(1):480-487. doi: 10.1021/acs.est.3c04495.

[37] Halder A, Gharami S, Sadhu P, Singh PK, Woźniak M, Ijaz MF. Implementing vision transformer for classifying 2D biomedical images. Sci Rep. 2024 May 31;14(1):12567. doi: 10.1038/s41598-024-63094-9. PMID: 38821977; PMCID: PMC11143185.

[38] Bazi, Y., Bashmal, L., Rahhal, M. M. A., Dayil, R. A., & Ajlan, N. A. (2021). Vision Transformers for Remote Sensing Image Classification. *Remote Sensing*, *13*(3), 516. https://doi.org/10.3390/rs13030516.

[39] N. Yadav, S. K. Singh and D. Sharma, "Forecasting Air Pollution for Environment and Good Health Using Artificial Intelligence," *2023 3rd International Conference on Innovative Sustainable Computational Technologies (CISCT)*, Dehradun, India, 2023, pp. 1-5, doi: 10.1109/CISCT57197.2023.10351334

[40] Li, J., & Luo, X. (2023). A Study of Weather-Image Classification Combining VIT and a Dual Enhanced-Attention Module. *Electronics*, *12*(5), 1213. https://doi.org/10.3390/electronics12051213

Appendix A

AQI	Air Quality Index
FTIR	Fourier Transformer Infrared Spectroscopy
CPCB	Central Pollution Control Board
Phyllotaxy	The pattern of leaf arrangement that provides morphological indicators of deposition
Wavenumber	The number of wave cycles per unit distance is known as a wave's spatial frequency.
Absobance	Absorbance (abbreviated as A) in spectroscopy is a logarithmic value that characterises the portion of a light beam that does not pass through a substance.
HPCB	Haryana Pollution Control Board
ViT	Vision Transformer
WHO	World Health Organisation
APTI	Air Pollution Tolerance Indices
NAQI	National Air Quality Index
DN	Digital Number
RMSE	Root Mean Square Error
BO-MLR	Baysian Optimized Multilevel Regression
R2	The coefficient of determination
$PM_{2.5}$	Particulate Matter, with $PM_{2.5}$ referring to particles(2.5) micrometers or smaller,
PM_{10}	Particulate Matter, with PM_{10} referring to particles (10) micrometers or smaller.
SO_2	Sulfur Dioxide a gas that can be released from industrial processes and fossil fuel combustion.
NO_2	Nitrogen Dioxide produced from burning fossil fuels in vehicles and power plants.
O_3	Ozone, a gas that can form both at ground level (a major component of smog) and in the upper atmosphere.